

Article

# Acoustic Identification of Turbocharger Impeller Mistuning—A New Tool for Low Emission Engine Development

Václav Pištěk <sup>1,\*</sup> , Pavel Kučera <sup>1</sup> , Oleksij Fomin <sup>2</sup> , Alyona Lovska <sup>3</sup> and Aleš Prokop <sup>1</sup>

<sup>1</sup> Institute of Automotive Engineering, Brno University of Technology, Technická 2896/2, 616 69 Brno, Czech Republic; kucera@fme.vutbr.cz (P.K.); prokop.a@fme.vutbr.cz (A.P.)

<sup>2</sup> Department of Cars and Carriage Facilities, State University of Infrastructure and Technologies, Kyrylivska str., 9, 04071 Kyiv, Ukraine; fomin\_ov@gsuite.duit.edu.ua

<sup>3</sup> Department of Wagons, Ukrainian State University of Railway Transport, Feuerbach sq., 7, 61050 Kharkiv, Ukraine; alyonalovskaya@kart.edu.ua

\* Correspondence: pistek.v@fme.vutbr.cz; Tel.: +420-541-142-271

Received: 28 August 2020; Accepted: 11 September 2020; Published: 14 September 2020



**Featured Application:** The acoustic method for identification of bladed disc mistuning described in this work will be useful for accelerating the development of new turbochargers and other impeller machines while significantly reducing costs.

**Abstract:** At present, exhaust gas turbochargers not only form the basis for the economical operation of petrol, diesel or gas engines of all power categories, but also have an irreplaceable role on reducing their emissions. In order to reduce emissions from internal combustion engines, various systems are being developed, all of which have a turbocharger as an important component. Demands on turbocharger system durability and reliability keep growing, which requires the application of increasingly advanced computational and experimental methods at the development beginning of these systems. The design of turbochargers starts with a mathematical description of their rotationally cyclic impellers. However, mistuning, i.e., a slight individual blade property deviation from the intended design parameters, leads to a disturbance of the rotational cyclic symmetry. This article deals with the effects of manufacturing-related deviations on the structural dynamic behaviour of real turbine rotors. As opposed to methods exploiting expensive scanning vibrometers for experimental modal analysis or time-consuming accurate measurement of the geometry of individual blades using 3D optical scanners. A suitable microphone and a finite element rotor wheel model are the basis of this new method. After comparing the described acoustic approach with the laser vibrometer procedure, the results seemed to be practically identical. In comparison with the laser technique the unquestionable added value of this new method is the fact that it brings a significant reduction in the financial requirements for laboratory equipment. Another important benefit is that the measuring process of bladed wheel mistuning is significantly less time-consuming.

**Keywords:** turbocharger; impeller; internal combustion engine; laser-measurement; microphone; modal hammer; Fourier Transform; FEM-model

## 1. Introduction

The compressor of an internal combustion engine turbocharger is usually designed as a radial flow stage. This enables compressor pressure ratios greater than six in single-stage operation. On the turbine side, impellers with radial or axial flow and their mixed-flow variants are used. Overlapping in the field of application, radial or mixed-flow turbines can guarantee high pressure ratios of the charger

with a small installation space, especially in the range up to 5000 kW. Especially for the latter case, there are requirements for ever-increasing mass flows. The specific swallowing capacity of the stage has to increase, which generally requires very long and thin blades. On the turbine side in particular, this poses special challenges for the structural dynamic design. On the one hand, the increased number of possible resonance points of the blading must be considered. Nevertheless, it is necessary to keep in mind that the aerodynamic damping to be expected during operation is low in comparison to the compressor. As a result, the phenomenon of mistuning comes into focus. Mistuning is caused by manufacturing-related deviations, through which the rotational cyclic design of the impellers is lost. The dynamic behaviour can thus significantly differ from the results obtained by an ideal impeller finite element model (FE), which among other things can lead to unexpectedly high blade stresses and premature component failure [1].

While the influence of the mistuning on compressor impellers in axial design has been sufficiently investigated in recent years, the topic for turbochargers and especially for radial turbines has only recently gained importance. It is precisely for this reason that a detailed examination of the vibration behaviour of real radial turbine wheels offers a possibility to further improving the robustness of these highly stressed components in relation to the cyclical fatigue of the blading.

Based on the description of the dynamic behaviour of rotational cyclic structures in [2,3], the term mistuning first appeared in scientific publications in the middle of the last century. The works [4–6] are undoubtedly the starting point for ongoing research activities in the areas of model building of mistuned bladed discs. Publication [5] investigates the mistuning effects of a blade using the example of a ring-shaped blade cascade. This upper limit only depends on the number of blades  $N$  and is often referred to as the Whitehead factor. This is based on the restrictive assumptions that only one blade is mistuned, all node diameter vibration modes are damped equally and, moreover, the coupling forces are lower than the damping forces. The fact that the complexity of the problem of describing the real bladed disc vibration behaviour can only be visualized to a small extent is demonstrated by the large number of scientific publications that have followed Whitehead's fundamental research to date.

Later research [1,6,7] shows magnification factors close to the Whitehead estimated limit, the publications use optimization strategies in order to mistune the system parameters in such a way that the greatest possible magnifications result. Author [8] refines the use of such optimization strategies, starting with a Monte Carlo simulation. Experimental examples with six and twenty-four blades show that [8] with values 1.61 and 2.81 approaches the Whitehead limit.

Author [9] is moving the solution forward to find the maximum magnification factor. His work also includes aerodynamic damping and shows that values above the Whitehead limit can result. Researchers [10] also investigate the size of the largest possible magnification factor taking aerodynamic damping effects into account, a genetic algorithm is used for the optimization.

Basic works describing the physical relationships of various parameters and their influence on the stress magnification that occurs are [11–13]. They establish the connection between the degree of coupling, mode localization phenomenon and magnification. Authors [11] use a simple spring-mass-damper system for this, whereas in [13] additional experiments are presented. The basic knowledge of both works is that blade mode shapes, which are characterized by weak coupling over the disc, tend to localize strongly.

In the recent past, through [14,15] attempted to find an upper limit for the expected stress magnification due to the mistuning. The latter authors included in their considerations the possibility of vibration mode modal coupling. In doing so, they relate the maximum magnification factor to the number of active modes, i.e., modes involved in the oscillation process. Researchers [16] also set an upper limit for the magnification. In addition to the coupling of the vibration modes, this also depends on the degree of mistuning and damping. In particular, for modes that occur in isolation, there are significantly lower values for the expected magnification compared to [5,15].

In the past decade [17] has dealt with this topic in radial turbines. In this article, the author contrasts several options for structurally dynamic description of the vibration behaviour of mistuned turbines.

Among other things, he describes a method using Lagrange multipliers. The model described here shows qualitative conformity in comparison to the experimentally determined vibration behaviour of the real turbine wheel.

Researcher [18] is concerned with the vibration stress calculation of the of radial turbine impellers, taking into account component real geometries. Based on the findings from the optical measurement of three turbine impellers, he defines the blade height, the blade angle and the blade thickness as varying parameters and examines their influence on the dynamics of the mistuned impeller. In addition, he compares this with the system behaviour with only variation of the elastic moduli of the blades. He concludes that the modelling of these pure stiffness shifts for simple mode shapes provide almost equivalent results compared to the models with geometric deviations. Differences in the calculated stress of up to 40% only occur with higher eigenfrequencies with complex mode shape types.

In their works, authors [19,20] investigate dynamics of very small radial impellers, using the results of the research works [21,22]. Many of the effects described therein are also confirmed using the example of these impellers with extremely small dimensions and very high-frequency vibrations. However, ref. [20] also states that the cast grain structure of this size has a significantly greater effect on the mistuning than with larger impellers. In addition, remarkable are the frequency deviations of individual blades of milled turbine impellers shown in [20], which amount to  $\pm 5\%$  there. Research papers [23–25] deal with the issue of impeller mistuning using the tip-timing method. The modal properties of real impellers also significantly affect the aero-acoustic properties of turbochargers, jet engines and fans which can currently be solved by advanced computational models [26,27].

Mistuning causes a significant reduction in the reliability and service life of turbocharger components in real operation. Due to the wide operating speed range of a turbocharger, only the computational determination of safety at individual resonant rotor speeds is difficult. The vibration resistance of newly developed turbochargers is therefore also verified in detail by technical experiments in test laboratories.

Mistuning of turbine impellers of various types can only be investigated experimentally. The main possible typical approaches have been mentioned above. Some authors use laser scanning vibrometer systems for experimental modal analysis which is a very expensive laboratory equipment [23–25,28]. Researchers [29,30] describe a more efficient method for identifying of the impeller mistuning, which uses only a one-beam laser. This method assigns the respective mode shapes calculated by an impeller FE model to individual peaks of measured transfer functions between the point of the force pulse of the modal hammer and the point where a vibration response is measured with a laser vibrometer.

The essence of the acoustic method presented in this paper is to replace the laser vibrometer with an appropriately sensitive microphone and to find the impeller eigenfrequencies and their corresponding mode shapes for individual blades using the measured acoustic response signal of the vibrating blade. The turbocharger impeller of a large industrial twenty-cylinder diesel engine was selected as the first research object, its outer and inner diameter is 260 mm and 140 mm, see Figure 1. The aim of the research was to examine in parallel the mistuning of the turbine impeller using this new method and a laser vibrometer and the subsequent comparison of the results.



**Figure 1.** Turbocharger radial turbine impeller of an industrial twenty-cylinder diesel engine.

## 2. Computational Modelling of Tuned Bladed Wheels

Essential information about the vibration properties of a particular tuned rotor can be provided by a suitable computational model based on the finite element method. Based upon a FE dynamic model of an impeller, the equation of motion in a rotating coordinate system is:

$$M\ddot{y} + (G + K)\dot{y} + Cy = f \tag{1}$$

where  $M$ —mass matrix,  $G$ —gyroscopic matrix,  $K$ —structural damping matrix and  $C$ —stiffness matrix. Vector  $y$  represents displacements and rotations at nodes and  $f$  the external forces. The stiffness matrix contains centrifugal stiffness and softening effects resulting from the static analysis under centrifugal, thermal and gas loads. In a non-rotating state, the bladed rotor system eigenvalues and eigenmodes can be found by solving the generalized eigenvalue problem.

Due to the cyclic periodicity of the ideal rotor geometry, the system matrices contain a block cyclic structure. Therefore, the resulting eigenvalues contain pairs of double modes.

In the case of bladed discs, complicated mode shapes often arise, the character of which is often difficult to specify only on the basis of a geometric shape or visualization by an animation program. The distribution of the specific strain energy in the mechanical structure of the impeller can be used for an objective assessment of the type of mode. Mode shapes having the specific strain energy contained in the blades more than 90% can be considered blade dominated. Mode shapes in which the value of the specific strain energy in the blades lies between 90% and 65% can be considered mixed. For specific strain energy values in the blades less than 65%, these are disc dominated mode shapes.

Strain energy is defined as the energy stored in a body due to deformation. Using the Hooke’s stress–strain law

$$\sigma = D\varepsilon, \tag{2}$$

the strain energy of the whole impeller structure is given by the volume integral

$$U = \frac{1}{2} \int_V \sigma^T \varepsilon dV = \frac{1}{2} \int_V \varepsilon^T D \varepsilon dV. \tag{3}$$

Within the discretization of the FE model is the integral reduced to the strain energy sum of all elements of the impeller. The energy distribution of the considered mode shape in the blade or in the disc or shaft body of the impeller structure is available to determine the dominant character of the eigenmode.

The rotationally cyclic symmetric impeller structure has similar mode shapes as a simple circular disc, but the number of nodal diameters  $ND$  is not unlimited. These so-called cyclic symmetric modes are characterized by the number of nodal diameters, their maximum number is:

$$ND = 0, 1 \dots \frac{N}{2}, \text{ if } N \text{ is even} \tag{4}$$

$$ND = 0, 1 \dots \frac{N-1}{2}, \text{ if } N \text{ is odd} \tag{5}$$

The eigenfrequencies of the mentioned mode shapes exist in pairs except of  $ND = 0$  and  $ND = N/2$ . These double modes have identical eigenfrequencies and only differ in the angular alignment of the nodal lines.

When creating finite element models of an impeller, the use of rotational cyclic symmetry is effective. In an ideal impeller, all blade sectors are geometrically identical and they have the same mechanical properties, so that their stiffness matrices are also identical. Due to the fact that the impeller is a rotationally cyclic symmetric elastic body, a computational numerical modal analysis can be performed for only one segment, and the modal analysis results for the whole structure can subsequently be obtained by using exact mathematical relations [28]. Figure 2 shows the finite element

model of one segment and the FE-mesh of the whole turbine impeller. The appropriate type and size of the element used for the computational FE-model were carefully determined by a series of comparative calculations.

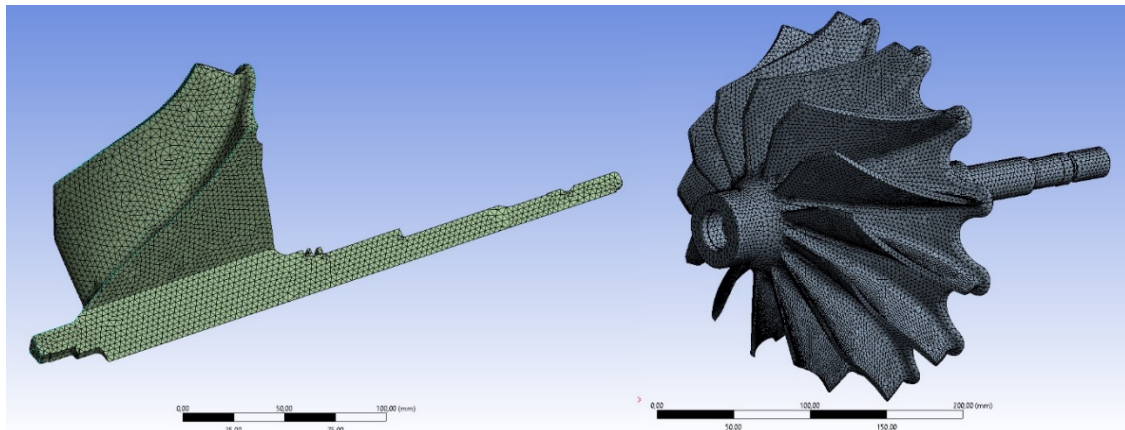


**Figure 2.** Finite element model of one segment and the model of the whole impeller.

The blade segment FE mesh was created at a special preprocessing software and it had to be done thoroughly in connection with the subsequent creation of a rotational cyclic model. There, it is important to properly connect the nodes on both sides of the segment to create the whole impeller rotational cyclic model. At the same time, it is necessary to achieve just the same segments that are really connected correctly. Shell and solid finite elements with a size of 3 mm were used on surfaces and inside the body up to 7 mm. The solver type was set automatically by the finite element software used.

The turbocharger rotors are usually mounted on two radial plain or roller bearings and one bearing is used to limit axial movements. The influence of bearings on blade dominated vibrations is negligible. It is therefore possible to set the so-called “free–free” boundary conditions for the computational modal analysis of the turbine impeller.

### 3. Arrangement of the Laboratory Experiment

The proposed technical experiment was carried out in an anechoic chamber, see Figure 3. The turbine wheel was installed on a very elastic mounting, so that the boundary conditions in the calculation and measurement match as much as possible. A force pulse at a suitable location on the blade was realized using a miniature modal hammer with a force sensor. The laser vibrometer measured the blade tip vibration speeds and the sound pressure was recorded synchronously using a measuring microphone.

To separate the vibrational movement of the measured blade, all other blades are additionally detuned by connecting weights of suitably selected size to the tips of the blade, as shown in Figure 4. The appropriate size of the additional weights in terms of shifting the natural frequencies of the unmeasured blades can be determined using the FE blade model of Figure 2. Several elements of the mass point type can be connected to the nodes at the considered place for connecting weights and their suitable mass can be determined by a few simple iterations.

The force pulse of the miniature modal hammer excites the blade to vibrate, while the laser vibrometer measures the vibration speed at the blade tip and the measurement microphone synchronously measures the sound pressure. The manual use of the modal hammer to create a force pulse on the blade presupposes a certain dexterity from the user. The designated suitable place for the modal hammer blow was color-coded on all blades and slight deviations from this point are not a problem. However, more severe distortion of the response signal occurs when a modal hammer blow is twice, which sometimes occurs with manual use. Therefore, the developed software also included a

double-blow check, and such records were excluded from further processing. The force pulse course of the used miniature modal hammer ensures that the frequency components of at least to 20 kHz will be captured in the measured response. For further research in this area, the authors have prepared a proposal for a mechanism that will replace the human hand, which will significantly improve the repeatability both the place and the force pulse course.



**Figure 3.** Arrangement of measurement techniques in an anechoic chamber.



**Figure 4.** Impeller with added masses ready for measurement and the miniature modal hammer.

The blade vibration measurements were carried out with and without additional weights on the blade tips, which confirmed their positive effect.

To record the measured data from the laser vibrometer and the measuring microphone, our own program modules were created. From more modal hammer force impulse response records, five were selected for frequency analysis using fast Fourier transform (FFT), and the results were averaged. Exponential windows [28] were used in modal impact testing to ensure the responses of the laser vibrometer and measuring microphone decay to zero within the measurement time to avoid leakage issues (see Figures 5 and 6). The used exponential window always starts at a value of 1.0 at the beginning of the measurement. The exponential decay parameter, a value between 0% and 100%, determines how much the initial value of the exponential window will be reduced at the end of the measurement.

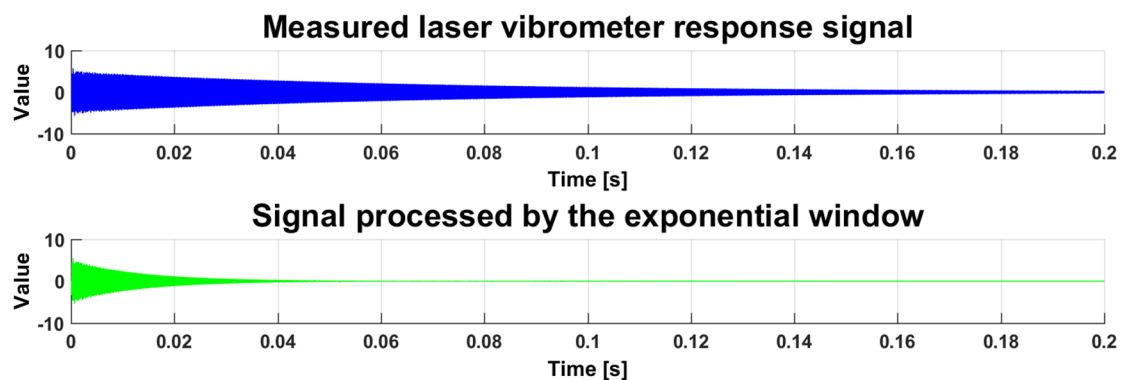


Figure 5. Impeller blade response to modal hammer force impulse—laser vibrometer measurement.

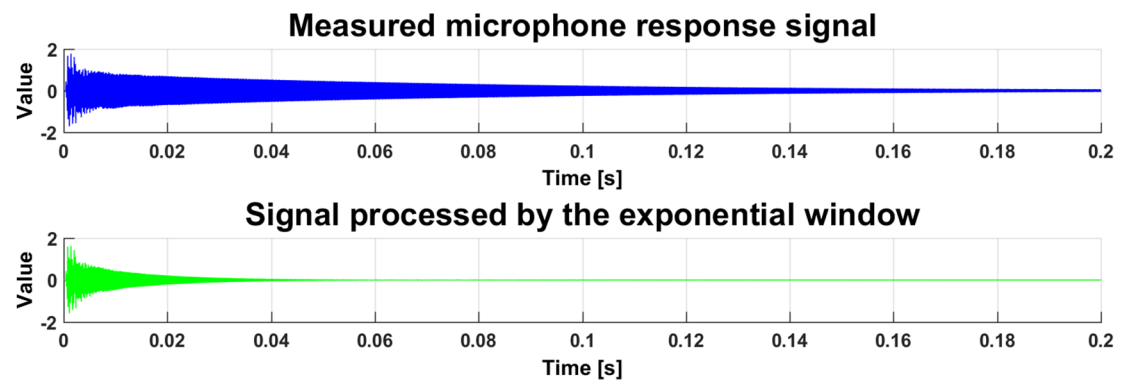


Figure 6. Impeller blade response to modal hammer force impulse—microphone measurement.

The time response recordings were 0.2 s, so the FFT frequency resolution was 5 Hz, which fully met the needs of the technical experiment.

#### 4. Results of the Acoustic method for Mistuning Identification

##### 4.1. Computational Finite Element Model of the Turbine Impeller

The computational finite element model of one impeller segment used for its modal analysis is shown in Figure 2 left. For this sub-model, the boundary conditions were specified as zero displacements and zero rotations in all three coordinate axes for nodes at both edges. Thus, the eigenfrequencies and their mode shapes associated with the impeller blade were obtained. Some selected examples are shown in Figure 7.

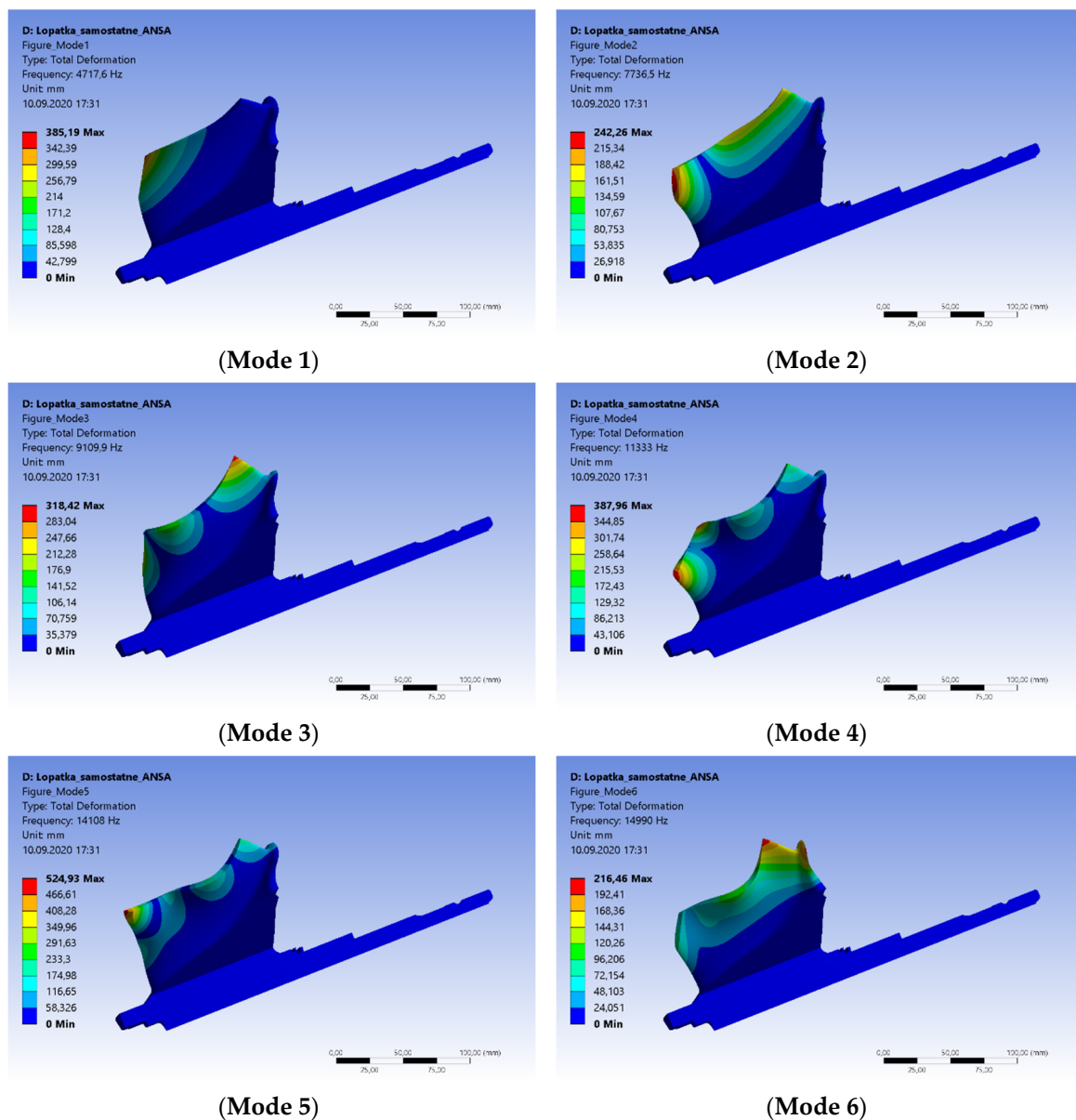


Figure 7. The first six blade mode shapes of the impeller segment.

The calculated turbine blade segment eigenfrequencies are shown in Table 1. Due to the value of the maximum impeller speed, the eigenfrequencies were investigated in the frequency range up to 20 kHz, which was also the frequency range of the measuring microphone used.

Table 1. Calculated eigenfrequencies of the impeller blade segment.

Mode (–)	Frequency (Hz)
1	4718
2	7737
3	9110
4	11,333
5	14,107
6	14,990
7	18,511

These eigenfrequencies determine approximately the ranges of values where the blade-dominated mode families will be located for the entire impeller.

The created mesh of the finite element model according to Figure 2 was further used to build a tuned rotational cyclic model of the whole turbine impeller. Its result is a nodal diameter map of the tuned impeller. Given the main topic of this article, these results are not presented in more detail.

Using the rotation of one segment, a 3D finite element model of the turbine wheel was subsequently created, the mesh of which is identical to the rotational cyclic model. Detailed calculations have verified that the results of the modal analysis of the 3D impeller model and the rotationally cyclic model are completely identical, the values of all calculated eigenfrequencies are the same to at least two decimal places

This model will continue to be used for analysis with different material properties of the blades and for studying the mistuning effect and for research of dangerous stress concentrators due to different characteristics of the individual blades. Figure 8 shows examples of the blade-dominated mode shapes of Modes 1–6. Due to the rigid structure of the impeller disc examined, there are no disc dominated mode shapes in the frequency range to 20 kHz. Instead, the vibration behaviour is determined by blade dominated and mixed mode shapes.

In the context of the blade vibrations of turbochargers, the analysis of the blade dominated mode shapes is of interest since unsteady pressure fluctuations in operation excite mainly just these. Examples of two different types of bladed wheel vibrations are shown in Figure 9. It is striking that the optical comparison of the displacements provides little information about the type of vibration to which the respective mode shape can be assigned. Information on strain energy distribution is crucial for the correct classification of the mode type. In the case of Mode 1 it is a blade dominated shape, while in the case of Mode 6 it is a mixed mode (see Figure 9).

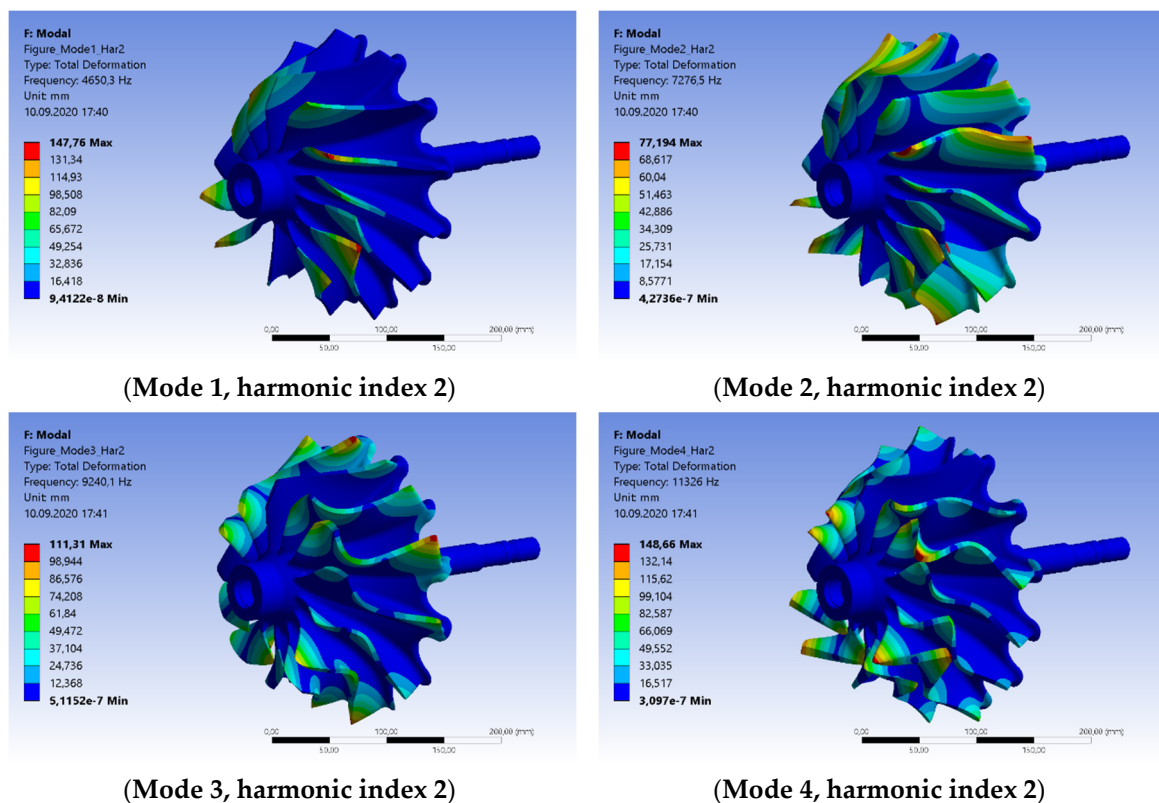


Figure 8. Cont.

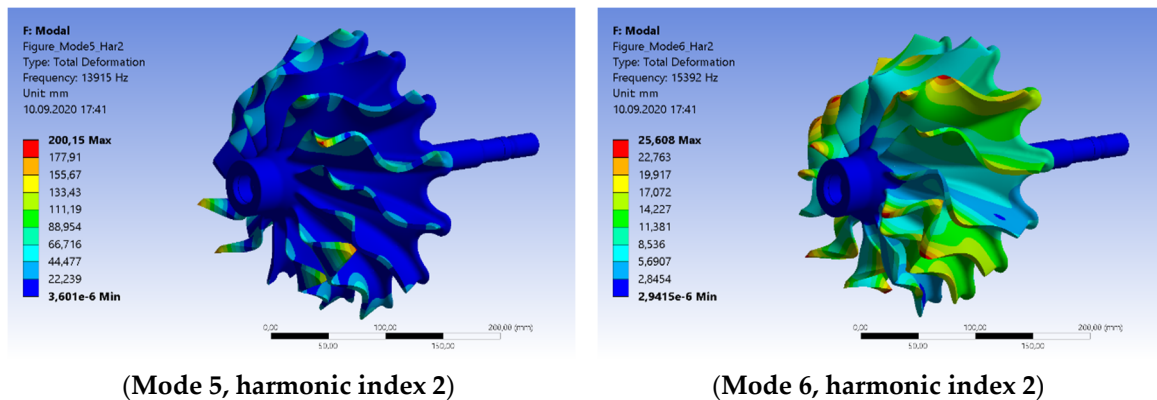


Figure 8. Some computed blade dominated mode shapes of the turbine impeller.

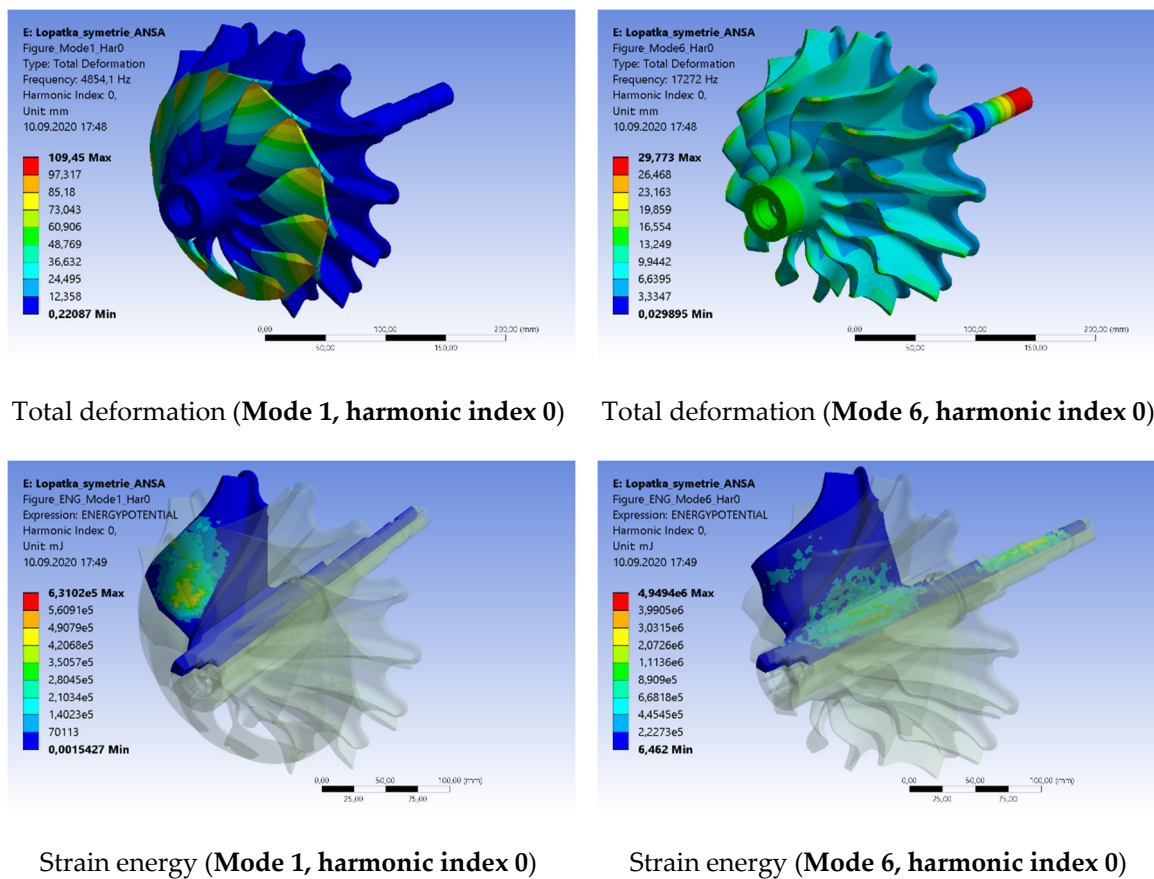
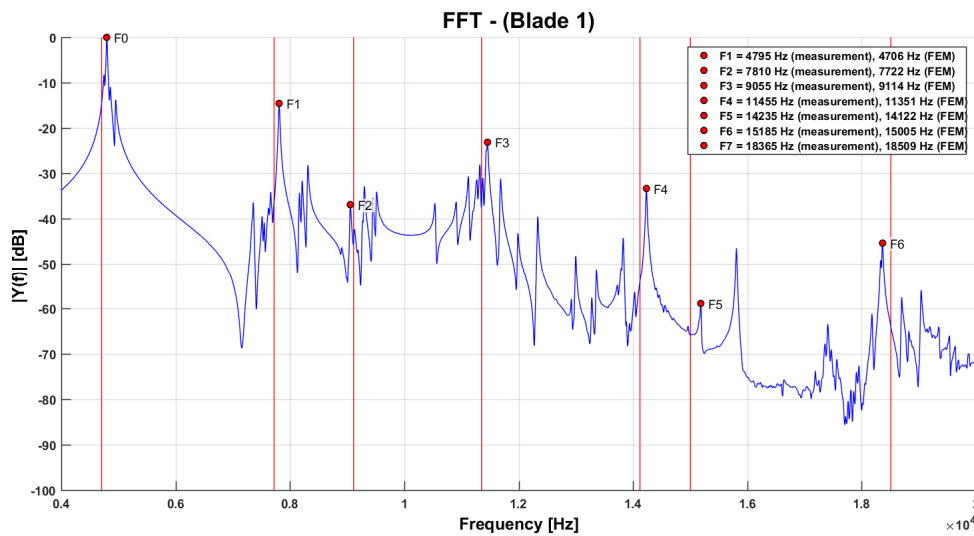


Figure 9. Examples of computed mode shapes and corresponding distribution of the strain energy.

#### 4.2. Measurement Results

For the individual blades, the FFT analyses of the measured responses from laser vibrometer and microphone were obtained. When measuring without additional weights on the other blades, the response also includes slightly different frequencies of the other mistuned blades, and it is practically impossible to evaluate the eigenfrequencies of the measured blade, see Figure 10.



**Figure 10.** Fast Fourier transform (FFT) analysis of measured response signal using the laser vibrometer and eigenfrequencies from the FE model—measured without additional weights.

The results of calculated FFT analysis of measured response signals of the first blade are shown in Figures 11 and 12. In this blade vibration measurement, weights were placed on other blade tips. When using a laser vibrometer, the frequencies of such detuned blades are significantly suppressed in the measured blade response. Similarly, by measuring with a microphone, repeated experiments have shown that with a suitable location of the microphone and due to its directional characteristic, the effect of detuned blades in the response of the measured blade is also negligible.

The additional weights with optimal size are very effective in suppressing the influence of the slightly different eigenfrequencies of the unmeasured blades. They make it possible to obtain the eigenfrequencies of individual blades of a real impeller and to create a mistuned 3D model for further detailed computational analysis. In Figures 11 and 12, red lines are drawn to indicate the eigenfrequencies of the one impeller segment from the FE simulation. A comparison of the measurement results of the methods using a laser vibrometer and a measuring microphone shows a good agreement of the results.

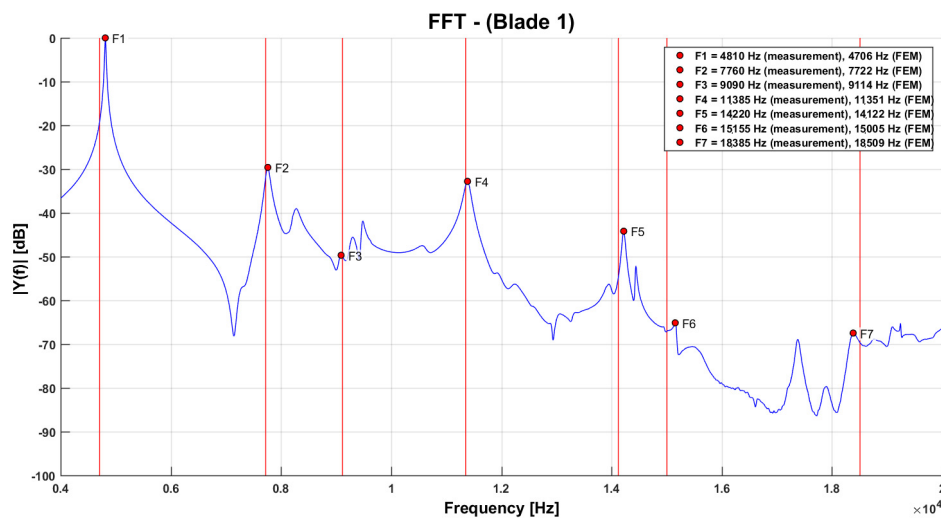


**Figure 11.** FFT analysis of measured response signal using the laser vibrometer and eigenfrequencies from the FE model—measured with additional weights.

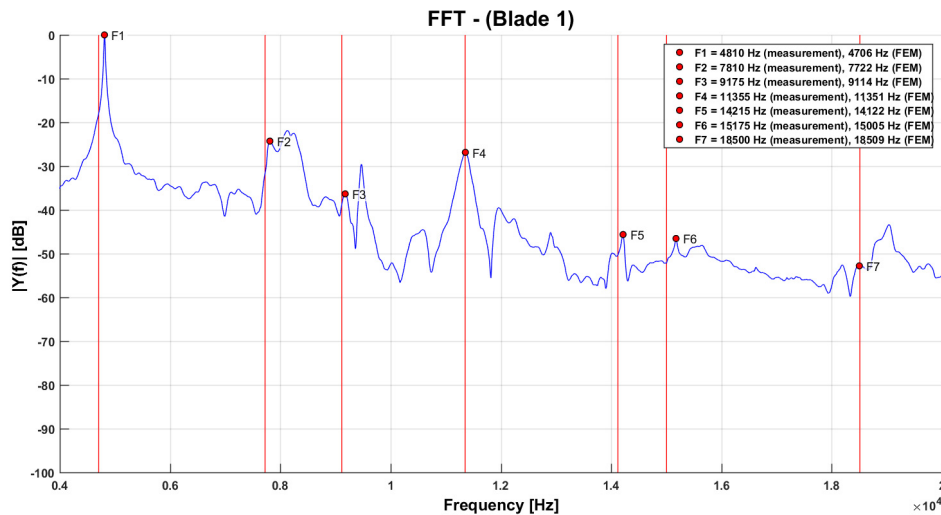


**Figure 12.** FFT analysis of measured response signal using the measuring microphone and eigenfrequencies from the FE model—measured with additional weights.

It is undoubtedly that the method using the FE model to assign the respective mode shapes to the individual peaks of the FFT analysis is suitable for further use with much simpler instruments than the use of an expensive single-beam laser or even a 3D scanning laser. Using this method, the user can only concentrate on the blade-dominated eigenfrequencies and does not have to pay attention to other FFT peaks that belong entirely or primarily to the turbine disk or shaft.

The size of the FFT spectral components in the measured response depends, when measured with a laser vibrometer or a microphone, among other things at the location of the force pulse on the blade. The location of the force pulse should not be close to the nodal lines of the blade mode shapes, but their position varies for each mode. Based on the results of the modal analysis of the blade, the location for the force pulse was chosen as a certain compromise. When it comes to choosing a measuring point for a laser vibrometer, the blade tip is a suitable place for all mode shapes. The F3 peak (Figure 11) can be highlighted and its presence confirmed by a more suitable location of the force pulse when measured by laser. The measuring microphone captures this F3 peak quite significantly already in the basic set-up of the experiment (Figure 12). However, the size of the individual detected frequency components in the measured response is not significant for the application of this method, whether it is measured by a laser vibrometer or a microphone.

Since the measured response was recorded in a time window of 0.2 s, the frequency resolution of the FFT is 5 Hz, and thus the uncertainty of the position of each spectral component on the frequency axis is 2.5 Hz, which is quite satisfactory for determining of the impeller mistuning.

From the performed measurements, similar diagrams as in Figures 11 and 12 were evaluated for all 13 blades of the turbine impeller. In the measured Fourier Transform analyses that represent a measure of the resonance amplitude, it is clearly visible that the eigenfrequencies  $f_i$  of the individual blades differ. The mistuning of the neighbouring blades is reflected in the relative eigenfrequency deviations

$$\Delta f_i = \frac{f_i - f_0}{f_0}, \quad f_0 = \frac{1}{N} \sum_{j=1}^N f_j \tag{6}$$

of all blades to one another. An example of the blade eigenfrequency mistuning of the measured impeller is shown in Figure 13. Describing the mistuning based on blade eigenfrequency deviations has the advantage that not all manufacturing tolerances of the impeller, for example deviations in shape or material inhomogeneity, have to be recorded individually. It is relatively difficult to find out in more detail the cause of the size of the mistuning of the individual blades, i.e., the extent to which material inhomogeneities or geometric deviations from the blade nominal dimensions contribute to this.

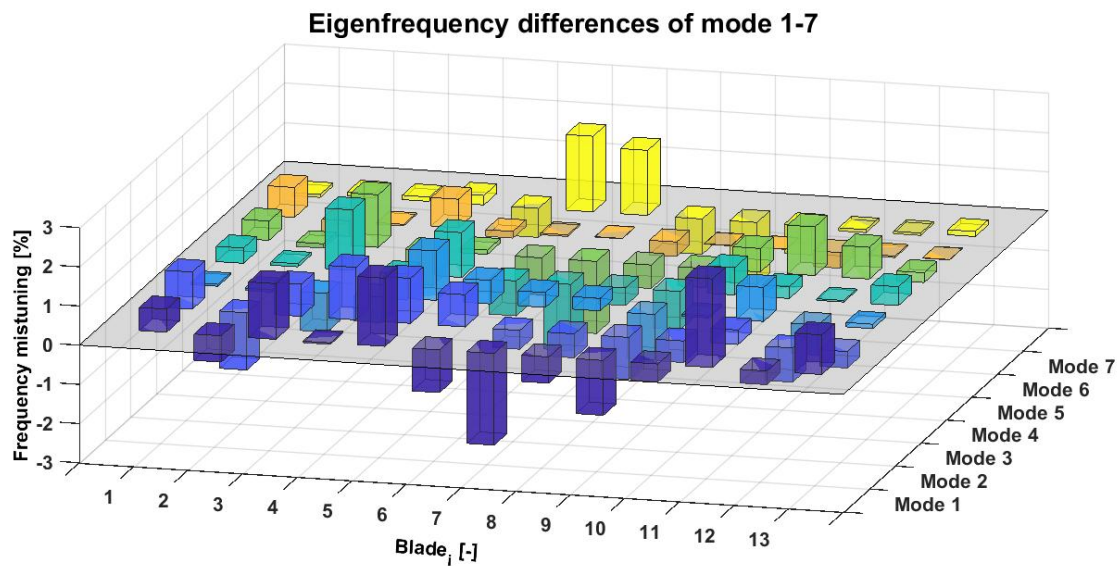


Figure 13. Eigenfrequency mistuning of turbine impeller blades of Modes 1–7.

In the case of the examined impeller, a scan of all the blades was subsequently carried out using an optical scanner. From the geometric model created in this way, deviations from the blade nominal dimensions according to the impeller Computer Aided Design (CAD) documentation were first determined. Subsequently, a 3D finite element model was created based on the determined actual geometry of the blades, the material parameters were considered the same throughout the model. Since the results of the computational modal analysis of this model showed good agreement with the measured values according to Figure 13, it is obvious that the main cause of this surveyed impeller mistuning are the geometric deviations of the blade profiles.

## 5. Conclusions

The article presented deals with the issue of the vibration of turbocharger impellers, in particular, with effective methods for determining their mistuning. The described acoustic method does not require the application of an expensive laser scanning techniques or a single-beam laser, but assigns the appropriate mode shapes to the individual detected peaks of the FFT analysis of the blade response using a computational finite element model. Simultaneously with the acoustic measurement, a laser vibration measurement at the blade tips was performed and the respective frequency analyses were evaluated. From a comparison of the FFT analysis determined by the acoustic method and the use of the laser vibrometer, it is obvious that both procedures lead to identical results.

A significant advantage of the presented acoustic method over laser Doppler vibrometry is its relative simplicity and considerably lower costs for measuring instruments. The computational model makes it easy to decide, among other things, what type of mode shape it is. In addition to showing the deformations of the impeller structure or animating the shape oscillation for individual modes, another important criterion is available. According to the distribution of specific strain energy in the sector of one blade calculated by finite element model, it is possible to decide whether it is a blade dominated, disc dominated or a mixed mode shape. Mode shapes in which the specific strain energy contained in the blades exceeds 90% can be considered blade dominated. Mode shapes in which the proportion of the specific strain energy in the blades is between 90 and 65% can be considered mixed. Mixed modes also occur in the impeller according to Figure 1, as shown by the results of the computational models and the results of the measurements, but they do not have a large effect on the stress in the blades. Disc-dominated modes were not detected in the investigated impeller which obviously follows from the robust design of the disc and the rigid connection of the blades to it. In the frequency spectrum evaluated from acoustic measurements, some peaks belonging to mixed

modes are highlighted compared to laser measurements. This can also be considered as a certain advantage over laser measurement in the case of bladed discs, in which resonant states corresponding to mixed or disc dominated modes would occur in the operating speed range. Similar measurements were performed for other cases of turbine wheels of various sizes, from turbochargers of diesel engines of heavy commercial vehicles to petrol engines of passenger cars. In all cases, the results of acoustic and laser measurements were found to be identical.

The presented acoustic method can therefore be considered as a full-fledged alternative to laser vibrometry, while the cost of the necessary measuring equipment is much lower. Its application compared to laser Doppler vibrometer measurement could be limited only in the case of very small impellers whose blade eigenfrequencies would exceed the measuring frequency range of the microphone used.

**Author Contributions:** Conceptualization, V.P.; methodology, V.P. and P.K.; software, P.K. and O.F.; validation, P.K., A.L. and A.P.; writing—review and editing, V.P. and P.K.; All authors have read and agreed to the published version of the manuscript.

**Funding:** The authors gratefully acknowledge funding from the Specific research on BUT FSI-S-20-6267.

**Acknowledgments:** The authors thank to Brno University of Technology for support.

**Conflicts of Interest:** The authors declare no conflict of interest.

## References

1. Petrov, E.P.; Ewins, D.J. Analysis of the Worst Mistuning Patterns in Bladed Disk Assemblies. *J. Turbomach.* **2003**, *125*, 623–631. [[CrossRef](#)]
2. Stodola, A. Über die Schwingungen von Dampfturbinen-Laufrädern. *Schweiz. Bauztg.* **1914**, *63*, 251–255.
3. Campbell, W. The protection of steam turbine disk wheels from axial vibration. *ASME Trans.* **1924**, *46*, 31–160.
4. Tobias, S.; Arnold, R. The influence of dynamical imperfections on the vibration of rotating disks. *Proc. Inst. Mech. Eng.* **1957**, *171*, 669–690. [[CrossRef](#)]
5. Whitehead, D.S. Effect of mistuning on the vibration of turbomachine blades induced by wakes. *J. Mech. Eng. Sci.* **1966**, *8*, 15–21. [[CrossRef](#)]
6. Ewins, D. The effect of detuning upon the forced vibration of bladed disks. *J. Sound Vib.* **1969**, *9*, 68–79. [[CrossRef](#)]
7. Rivas-Guerra, A.; Mignolet, M. Maximum amplification of blade response due to mistuning: Localization and mode shape aspects of the worst disks. *J. Turbomach.* **2003**, *125*, 442–454. [[CrossRef](#)]
8. Chan, Y. Variability of Blade Vibration in Mistuned Bladed Discs. Ph.D. Thesis, Imperial College London, London, UK, October 2009.
9. Petrov, E. Reduction of forced response levels for bladed discs by mistuning: Overview of the phenomenon. In Proceedings of the ASME TurboExpo, Glasgow, UK, 14–18 June 2010.
10. Beirow, B.; Kühhorn, A.; Giersch, T.; Nipkau, J. Optimization-aided forced response analysis of a mistuned compressor blisk. In Proceedings of the ASME TurboExpo, Düsseldorf, Germany, 16–20 June 2014.
11. Wei, S.T.; Pierre, C. Localization phenomena in mistuned assemblies with cyclic symmetry Part 1: Free vibrations. *J. Vib. Acoust. Stress Reliab. Des.* **1988**, *110*, 429–438. [[CrossRef](#)]
12. Wei, S.T.; Pierre, C. Localization phenomena in mistuned assemblies with cyclic symmetry Part 2: Free vibrations. *J. Vib. Acoust. Stress Reliab. Des.* **1988**, *110*, 439–449. [[CrossRef](#)]
13. Judge, J.; Pierre, C.; Mehmed, O. Experimental investigation of mode localization and forced response amplitude magnification for a mistuned bladed disk. *J. Eng. Gas. Turbines Power* **2001**, *123*, 940–950. [[CrossRef](#)]
14. Kenyon, J.; Griffin, J. Forced response of turbine engine bladed disks and sensitivity to harmonic mistuning. *J. Eng. Gas. Turbines Power* **2002**, *125*, 113–120. [[CrossRef](#)]
15. Martel, C.; Corral, R. Asymptotic description of maximum mistuning amplification of bladed disk forced response. *J. Eng. Gas. Turbines Power* **2008**, *131*, 1–10.
16. Figaschewsky, F.; Kühhorn, A. Analysis of mistuned blade vibrations based on normally distributed blade individual natural frequencies. In Proceedings of the ASME TurboExpo, Montreal, QC, Canada, 15–19 June 2015.

17. Irwanto, B. Schaufelschwingungsanalyse am Elastischen Beschaufelten Rotor: Numerische und Experimentelle Untersuchungen. Ph.D. Thesis, Technische Universität Dresden, Dresden, Germany, 2006.
18. Drozdowski, R. Berechnung der Schwingbeanspruchungen in Radialturbinenrädern unter Berücksichtigung realer Bauteilgeometrien. Ph.D. Thesis, Technische Universität Dresden, Dresden, Germany, November 2011.
19. Hemberger, D.; Filsinger, D.; Bauer, H.J. Mistuning modelling and its validation for small turbine wheels. In Proceedings of the ASME TurboEspo, San Antonio, TX, USA, 3–7 June 2013.
20. Hemberger, D.; Filsinger, D.; Bauer, H.J. Identification of mistuning for casted turbine wheels of small size. In Proceedings of the ASME TurboEspo, Düsseldorf, Germany, 16–20 June 2014.
21. Beirow, B. *Grundlegende Untersuchungen zum Schwingungsverhalten von Verdichterlaufrädern in Intergralbauweise*; Shaker Verlag: Aachen, Germany, 2009.
22. Beirow, B.; Kühhorn, A.; Figaschewsky, F.; Hönisch, P.; Giersch, T.; Schrape, S. Model Update and Validation of a Mistuned High Pressure Compressor. *Aeronaut. J.* **2019**, *123*, 230–247. [[CrossRef](#)]
23. Hattori, H. Study on mistuning identification of vehicle turbocharger turbine BLISK. In Proceedings of the ASME Turbo Expo 2014: Turbine Technical Conference and Exposition, Düsseldorf, Germany, 16–20 June 2014; pp. 1–10.
24. Rzadkowski, R.; Kubitz, L.; Maziarz, M.; Troka, P.; Dominiczak, K.; Szczepanik, R. Tip-Timing measurements and numerical analysis of last-stage steam turbine mistuned bladed disc during run-down. *J. Vib. Eng. Technol.* **2020**, *8*, 409–415. [[CrossRef](#)]
25. Fan, C.; Wu, Y.; Russhard, P.; Wang, A. An Improved Blade Tip-timing Method for Vibration Measurement of Rotating Blades during Transient Operating Conditions. *J. Vib. Eng. Technol.* **2020**. [[CrossRef](#)]
26. Velarde, S.; Tajadura, R. Numerical simulation of the aerodynamic tonal noise generation in a backward-curved blades centrifugal fan. *J. Sound Vib.* **2006**, *295*, 781–786.
27. Cravero, C.; Marsano, D. Numerical prediction of tonal noise in centrifugal blowers. In Proceedings of the Turbo Expo 2018: Turbomachinery Technical Conference & Exposition, Oslo, Norway, 11–15 June 2018; ASME Paper GT2018-75243.
28. Pawlenka, M.; Mahdal, M.; Tuma, J.; Burecek, A. Application of a Bandpass Filter for the Active Vibration Control of High-Speed Rotors. *Int. J. Acoust. Vib.* **2019**, *24*, 608–615. [[CrossRef](#)]
29. Píšťek, V.; Kučera, P.; Fomin, O.; Lovska, A. Effective Mistuning Identification Method of Integrated Bladed Discs of Marine Engine Turbochargers. *J. Mar. Sci. Eng.* **2020**, *8*, 379. [[CrossRef](#)]
30. Weber, R. Ein Beitrag zur schwingungssicheren Auslegung von radialen Turbomaschinen mit Fokus auf Mistuning und Dämpfung. Ph.D. Thesis, Mensch & Buch Verlag: BTU Cottbus-Senftenberg, Cottbus, Germany, May 2019.



© 2020 by the authors. Licensee MDPI, Basel, Switzerland. This article is an open access article distributed under the terms and conditions of the Creative Commons Attribution (CC BY) license (<http://creativecommons.org/licenses/by/4.0/>).